ARTICLE IN PRESS

ELSEVIER

Journal of Fluids and Structures ▮ (▮▮▮▮) ▮▮▮–▮▮▮

JOURNAL OF FLUIDS AND STRUCTURES

www.elsevier.com/locate/jfs

Energy criteria for elasto-capillary wrapping

E. de Langre*, C.N. Baroud, P. Reverdy

Department of Mechanics, LadHyX, CNRS-Ecole Polytechnique, 91128 Palaiseau, France

Received 3 February 2009; accepted 8 October 2009

Abstract

We consider the interaction between a liquid drop and a flexible membrane, a fluid–structure problem where capillarity is the dominant fluid contribution. Recent work has shown that surface tension may be used to bend an elastic membrane if the typical scale of the membrane is above a critical length. Here, we discuss some more detailed experimental measurements that demonstrate the switching between different modes of folding as well as a dewetting transition during the folding of the membrane. A model is then developed, based on an energy approach, and shown to account for all of the observed phenomena. Contrary to more refined modelling, the minimal model may be extended to more complex cases with little extra work, making it useful for complex geometries or in order to include further physical ingredients.

Keywords: Capillarity; Elasticity; Dewetting; Wrapping; Membrane

1. Introduction

Interactions between elasticity and capillary forces play a dominant role in many biological situations when liquid drops come in contact with soft tissue. In the human lung for example, the presence of liquid may cause the airway to collapse under the action of capillary pressure (Halpern and Grotberg, 1992; Heil, 1999). Capillary forces are also used by some fungi to store elastic energy which then serves to eject the spores (Ingold, 1971). In micro- and nano-technologies, the increasing role of surface tension as the length scales decrease can lead to unwanted phenomena, such as the stiction of MEMS structures or nano-tube carpets (Mastrangelo and Hsu, 1993; Lau et al., 2003; Raccurt et al., 2004).

Alternatively, the folding of two-dimensional mechanical structures by action of surface tension has recently been suggested as a method to produce three-dimensional micro- and nano-devices (Leong et al., 2006; Py et al., 2007). Indeed, the fabrication of three-dimensional micro-structures presents major challenges to the MEMS industry since most micro-fabrication processes rely on surface deposition and etching of a substrate, processes which can only lead to the stacking up of layers. The fabrication of truly three-dimensional shapes such as hollow tubes or spheres remains a challenge (Madou, 2002).

One approach which has recently been gaining popularity is to fold a two-dimensional structure into a three-dimensional object. This technique, referred to as *micro-origami*, can rely on a variety of approaches to fold the solid

*Corresponding author.
E-mail address: delangre@ladhyx.polytechnique.fr (E. de Langre).

0889-9746/$ - see front matter © 2009 Elsevier Ltd. All rights reserved.
doi:10.1016/j.jfluidstructs.2009.10.004

Please cite this article as: de Langre, E., et al., Energy criteria for elasto-capillary wrapping. Journal of Fluids and Structures (2010), doi:10.1016/j.jfluidstructs.2009.10.004

substrate. One approach is to use multiple solid layers and to actuate surface stresses with optical or chemical techniques [see for example Smela et al. (1995); Ocampo et al. (2003)], while others have relied on the surface tension of solder to position independent blocks of metal, and then hold them once solidified (Syms et al., 2003; van Honschoten et al., 2009).

In the case of elastic 2-D sheets, recent experiments have shown that the competition between surface tension and elasticity can turn in favour of surface tension at small scales (Py et al., 2007). Indeed, a drop of water that is deposited on a thin flexible membrane was shown to produce large deformations in the membrane, sometimes leading to complete encapsulation of the liquid by the solid. Different initial shapes of the flat membrane were shown to produce different final configurations, providing the ability to design *a priori* the final shape of the encapsulated liquid by cutting the membrane accordingly.

The wrapping of the drop by the membrane is only possible, however, if the energy gained from reducing the liquid–air surface area is larger than the energy cost of bending the elastic membrane. An order-of-magnitude scaling analysis may be used to demonstrate the existence of an elasto-capillary length $L_{EC}=[Eh^3/12(1-\nu^2)\gamma]^{1/2}$, which depends on the physical properties (Young's modulus E, Poisson's ratio ν) and geometry of the membrane (thickness h), as well as on the surface tension of the liquid that is used (γ). It was observed that the encapsulation could only occur if the typical dimension of the membrane was a few times L_{EC}.

Going beyond the scaling analysis is no simple matter; while it may be useful to have a coupled fluid–structure model which accounts for the large deformations, another approach is to develop a highly simplified description which can be solved by hand, in order to give the general trends without any computations. Indeed, we show below that a minimal model, which takes into consideration the most basic phenomena, can recover the results of the 2-D numerical simulations of Py et al. (2007). In addition to this, we show how it can be extended to more complex questions that arise in the experiments for which the numerical model would need to be greatly complicated.

We begin, in Section 2, by describing some new experimental observations. This is followed, in Section 3, by the model based on an energy approach which is then compared with the experimental observations of the present work and of Py et al. (2007).

2. New experimental observations

Two phenomena appear in the experiments that we describe below, in addition to the observations of Py et al. (2007): mode switching and dewetting.

The experiments were conducted by depositing a water drop on top of a thin membrane, which was made by spin-coating a layer of poly-dimethylsiloxane (PDMS) on a glass slide and manually cutting it out after curing. The final membrane was cut into a square, of a few mm in size and ranging in thickness between 40 and 80 μm. The membrane was placed on a rough, low-energy, surface in order to prevent adhesion with the substrate and to facilitate the drop manipulation. The water drop was then deposited using a micro-pipette and allowed to evaporate over the course of a few minutes, while a time lapse image sequence was acquired through a microscope. This yielded a history of the folding process.

Two simultaneous views were obtained at each image, as shown in Fig. 1, by placing a mirror at 45° next to the drop–membrane pair. The image of the drop on the bottom of the figure corresponds to the direct view through the microscope looking vertically down, while the image on the top is the reflection through the mirror. In this way, quantitative measurements were possible on two projection planes.

2.1. Mode switching

When the drop is first deposited on the membrane, the four corners of the square are lifted and pulled towards the centre of the drop, corresponding to the image in Fig. 1. In this configuration, the drop shape is closely approximated as a spherical cap, while the membrane displays an evenly distributed curvature, as seen by the gentle curve of the membrane edge on the mirror view.

The folding process is shown in Fig. 2. As the liquid begins to evaporate, the four corners are pulled towards the centre of the drop, keeping the square (mode IV) shape. However, this four-fold symmetry is eventually broken and the membrane relaxes to a mode II pattern where the corners are drawn together in pairs. The switching step between the two shapes happens faster than the frame rate that is used and is not resolved in our visualizations. In this mode II configuration, the system folds along a line parallel to two of the sides, with the curvature remaining well distributed in all regions of the membrane. The final shape, after the water has largely evaporated, is that of a tube with nearly

Please cite this article as: de Langre, E., et al., Energy criteria for elasto-capillary wrapping. Journal of Fluids and Structures (2010), doi:10.1016/j.jfluidstructs.2009.10.004

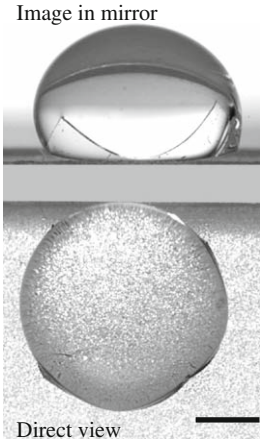

Fig. 1. Experimental image taken through the microscope. The drop–membrane is seen vertically on the bottom image, while a mirror provides a simultaneous side view. The granular texture below the drop is due to the super-hydrophobic surface. The scale bar represents 1 mm.

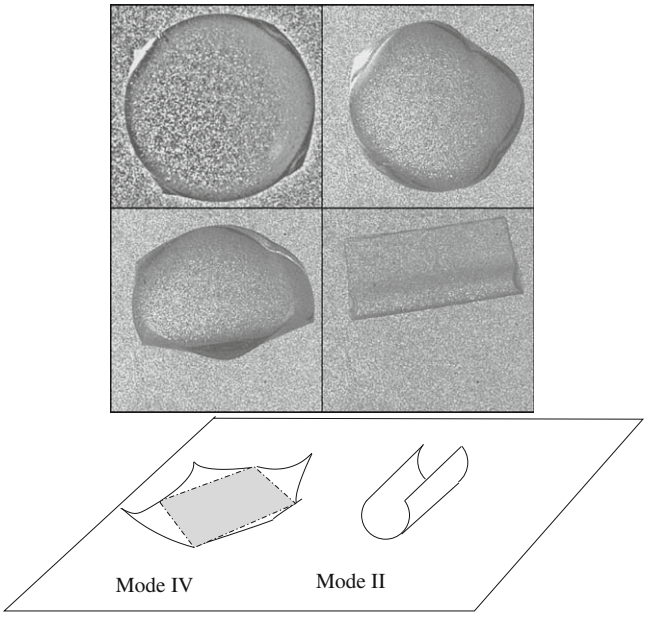

Fig. 2. The folding process of a drop on a square membrane, seen from above (top). Folding starts inmode IV, where the four corners bend, and ends in mode II (bottom).

constant cross-section. Note that the switching to a mode II that folds along the diagonal is possible if two diagonally opposed corners are rounded.

The evolution from a mode IV to II folding pattern can be quantified by following the four corners of the square during the drying up process. This is shown in Fig. 3(a) where the position of each of the corners is marked during the initial stages of the folding, until the onset of the mode switching. On this figure, the evolution from a square to a diamond shape is shown by graphically connecting the corners of the membrane at three successive characteristic times. The departure of the shape from a square is quantified by calculating the squareness $\mathrm{Sq} = 4A^{1/2}/L$, where A is the area enclosed between the four corners and L the perimeter of the four sided polygon defined by the corners (Fig. 3(b)). This ratio is equal to unity for a perfect square and should decrease from this value as the shape changes.

The switching away from mode IV can be observed in Fig. 3(b), where we have plotted the evolution of $\mathrm{Sq}(t)$ for two different experiments involving different membranes. We observe that the switching occurs abruptly after a long period

Please cite this article as: de Langre, E., et al., Energy criteria for elasto-capillary wrapping. Journal of Fluids and Structures (2010), doi:10.1016/j.jfluidstructs.2009.10.004

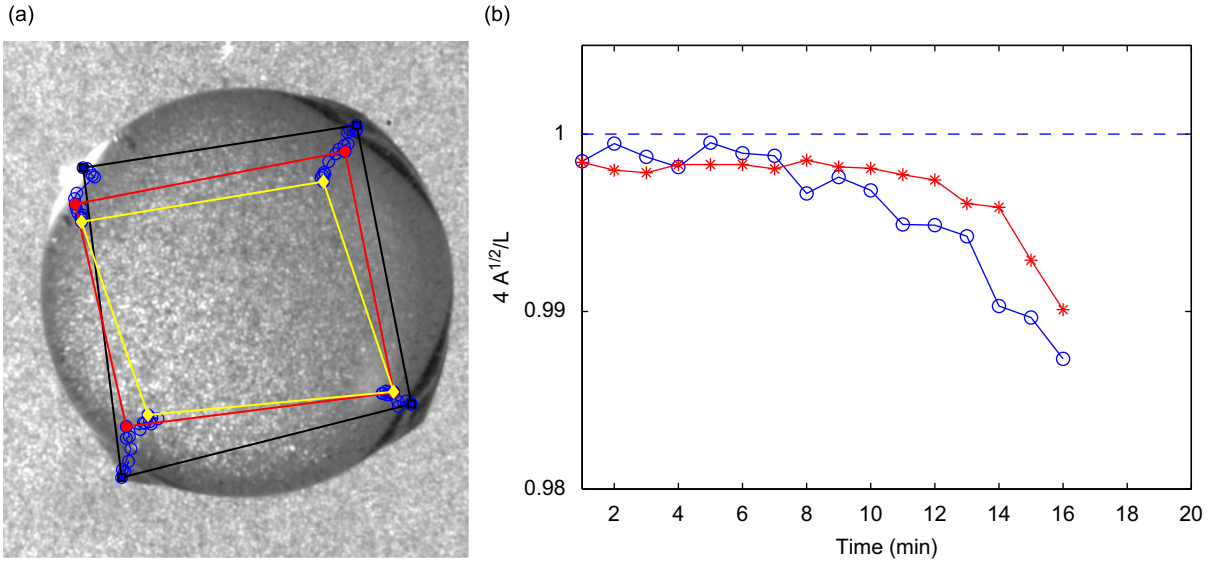

Fig. 3. (a) The position of the four corners at successive times and (b) evolution of the squareness ratio of $\mathrm{Sq} = 4A^{1/2}/L$ as the drop volume decreases with evaporation.

during which the ratio remains near 1. The later evolution of Sq cannot be followed since the membrane changes orientation and some of the corners get masked. However, this mode switching happens for all the square membranes, as well as with other shapes which begin with a mode IV symmetry, such as a four-petal flower.

2.2. Non-encapsulation through dewetting

When the membrane's characteristic length is smaller than L_{EC}, the membrane will never fully encapsulate the drop, as noted in Py et al. (2007). In this case, the evaporation process will generally lead to a thin film of liquid covering the membrane, which is almost flat, before this film fully evaporates.

A different mode of non-encapsulation may also occur when the liquid initially fails to fully reach the four corners and the likelihood of this situation increases as the membrane thickness increases. To understand this, recall that the total curvature on the drop surface, defined as the sum of the two principal curvatures $\kappa = \kappa_1 + \kappa_2$, must be uniform for the Laplace pressures to be balanced in the liquid. This requires that one principal curvature must decrease if the other principal curvature increases, in order to maintain an invariant total. However, a corner presents a singular point which requires infinite curvature in the plane of the membrane and this would have to be balanced by infinite negative curvature in the normal direction. This is achieved, in the case of a flexible membrane, by folding the membrane onto the drop, thus yielding very high curvature near the contact point. However, stiff membranes will fail to bend sufficiently and the corners of thick membranes may remain dry.

Fig. 4 shows the evaporation of such a drop. Rather than the standard process described in Py et al. (2007), this situation leads to progressive dewetting of the membrane which starts at the top left corner (which was imperfectly wetted) and eventually leaves a curved drop sitting on top of an almost flat membrane.

3. Energy criteria

3.1. Two-dimensional model

We now propose a simple model for estimating the domain of possible capillary wrapping. Three distinct states are found when evaporating a drop on a flexible membrane: either a wrapped state, denoted by W; a flat state denoted by F; or a dewetted state, denoted by D. These three states are illustrated in Fig. 5 in a simplified two-dimensional framework. They correspond to the same volume of fluid and we assume that the state that will be observed is that of minimum total energy. The volume of fluid we consider, S, is such that there is no free liquid–air surface in the wrapped state, as shown in

Please cite this article as: de Langre, E., et al., Energy criteria for elasto-capillary wrapping. Journal of Fluids and Structures (2010), doi:10.1016/j.jfluidstructs.2009.10.004

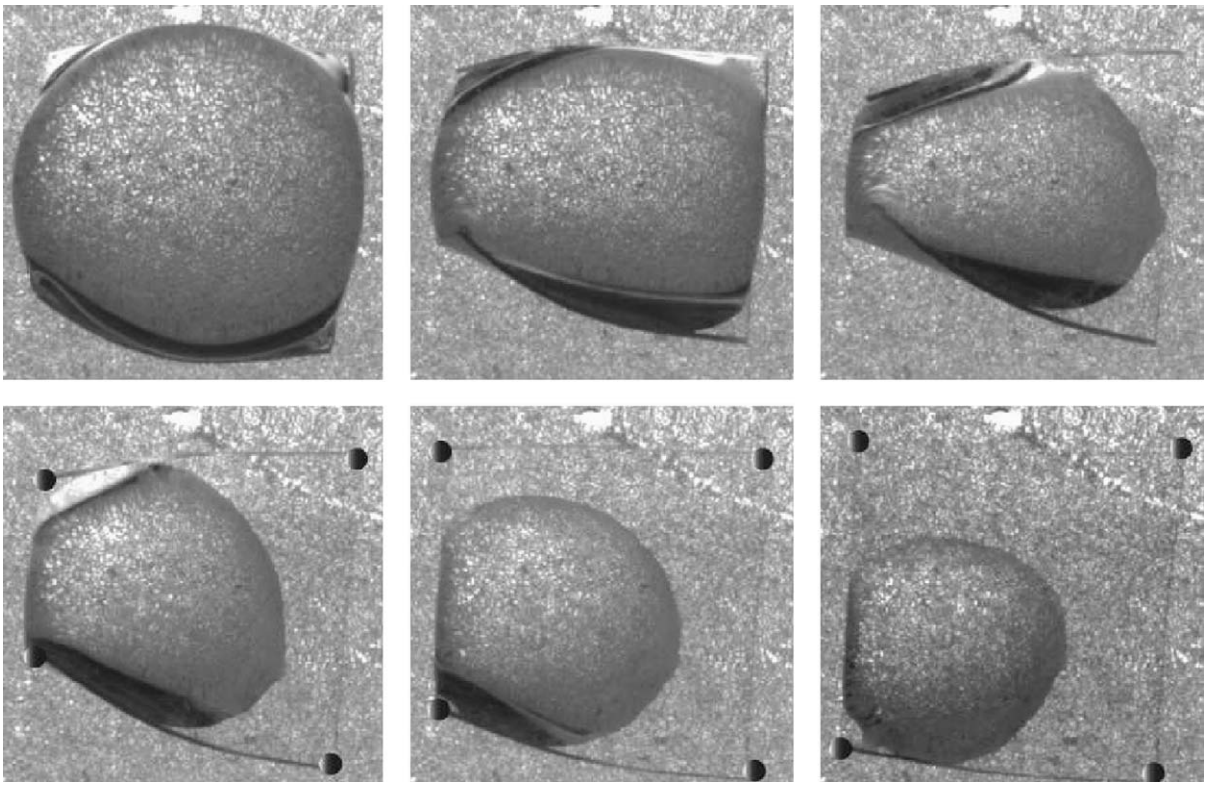

Fig. 4. A drop going through a typical dewetting situation during dry-up, from top left to bottom right. Time between images is about 2 min. The corners of the membrane are shown with black dots on the lower images, during the dewetting stage.

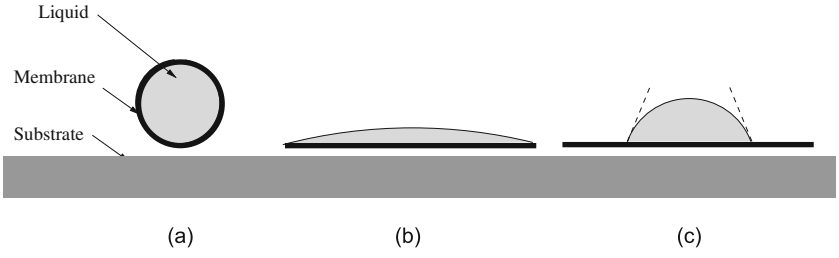

Fig. 5. Possible 2-D states for a membrane with a liquid: (a) wrapped state, (b) flat state, and (c) dewetted state.

Fig. 5(a). In that case we have a volume of fluid (actually a surface in this two-dimensional model), $S = L^2/4\pi$ where L is the length of the membrane.

The total energy E is given by the sum of the elastic bending energy, E_B, the capillary energy, E_C, and the gravity potential energy E_G. Note that we do not consider here the elastic energy associated with in-plane tension of the membrane. This is justified by the length to thickness ratio of the membranes L/h, which is always larger than 10: since the bending energy scales as $(L/h)^3$ while the in-plane tension energy scales as L/h, the latter may be neglected as long as the loading of the membrane is not purely in plane.

These energies are approximated using a schematic shape of the membrane and of the fluid surface, both of which we model as circular. The bending energy can be written as

$$E_B = \frac{1}{2} L \frac{B}{R^2}, \tag{1}$$

Please cite this article as: de Langre, E., et al., Energy criteria for elasto-capillary wrapping. Journal of Fluids and Structures (2010), doi:10.1016/j.jfluidstructs.2009.10.004

where B is the bending stiffness of the membrane and R is the radius of curvature. Let L' be the length of the free surface of the fluid. The capillary energy is

$$E_C = L'\gamma, \tag{2}$$

where γ is the surface tension. Finally, the gravitational potential energy is

$$E_G = \rho S g z, \tag{3}$$

where ρ is the density of the fluid and z is the vertical position of the centre of mass of the fluid. The mass of the membrane is neglected as being small compared to that of the fluid.

3.1.1. Wrapped state

In the wrapped state, Fig. 5(a), the area of free liquid surface is zero so that $E_C = 0$. Since the membrane is fully wrapped its radius of curvature is such that $2\pi R = L$, so that $E_B = 2L\pi^2 B/L^2$. Finally the centre of mass is at $z = R$. The total energy can therefore be expressed as

$$E^W = \frac{1}{2}L\left(\frac{4\pi^2 B}{L^2}\right) + \rho g \pi \frac{L^3}{8\pi^2}. \tag{4}$$

3.1.2. Flat state

In the flat state depicted in Fig. 5(b), the membrane stores no bending energy so $E_B = 0$ and the length of free liquid surface is such that it covers a volume equal to S over a distance L. Let r be the radius of curvature of the free liquid surface and 2θ the angle of the arc formed by this line. Then $L = 2r\sin\theta$, $L' = 2r\theta$ and $S = r^2(\theta - \sin\theta\cos\theta)$. Using the condition that $S = L^2/4\pi$, eliminating r and θ from these equations yields $L'/L = \alpha \simeq 1.0368$. The position of the centre of mass is also given by geometric considerations $z/L = \beta \simeq 0.0474$. The total energy in the flat state therefore reads

$$E^F = L\alpha\gamma + L\beta\rho g\frac{L^2}{4\pi}. \tag{5}$$

3.1.3. Dewetted state

Finally, in the dewetted state of Fig. 5(c), the geometry can be obtained from the known value of the receding contact angle θ. In that case the membrane is flat so that $E_B = 0$, while the length of free liquid surface is

$$\frac{L'}{L} = \alpha' = \sqrt{\pi(\theta - \sin\theta\cos\theta)}. \tag{6}$$

The position of the centre mass also depends on θ and can be expressed as

$$\frac{z}{L} = \beta' = \frac{1}{\pi\sqrt{\theta - \sin\theta\cos\theta}}\left[\frac{2\sin^3\theta}{(\theta - \sin\theta\cos\theta)} - \cos\theta\right]. \tag{7}$$

The total energy reads

$$E^D = L\alpha'\gamma + L\beta'\rho g\frac{L^2}{4\pi}. \tag{8}$$

3.1.4. Dimensionless forms of the energies

These results may be put in dimensionless form by introducing two characteristic length scales: the elasto-capillary length $L_{EC} = \sqrt{B/\gamma}$ and the traditional capillary length scale $L_C = \sqrt{\gamma/\rho g}$. The total energy of the three states discussed above is non-dimensionalized as $\mathcal{E} = EL/B$ and yields

$$\mathcal{E}^W = 2\pi^2 + \frac{1}{8\pi^2}\ell^4\lambda^2, \tag{9}$$

$$\mathcal{E}^F = \alpha\ell^2 + \frac{\beta}{4\pi}\ell^4\lambda^2, \tag{10}$$

and

$$\mathcal{E}^D = \alpha'\ell^2 + \frac{\beta'}{4\pi}\ell^4\lambda^2, \tag{11}$$

where we have used $\ell = L/L_{EC}$ and $\lambda = L_{EC}/L_C = \sqrt{B\rho g}/\gamma$, the latter being constant for a given membrane and fluid.

Please cite this article as: de Langre, E., et al., Energy criteria for elasto-capillary wrapping. Journal of Fluids and Structures (2010), doi:10.1016/j.jfluidstructs.2009.10.004

3.1.5. Phase diagram

Fig. 6 displays the lowest energy configuration as a function of the dimensionless length of the membrane, $\ell = L/L_{EC}$, and of $\lambda = L_{EC}/L_C$. We observe that the wrapped state only appears for small λ and large ℓ, i.e. in a finite range of membrane lengths for which the corresponding energy is less than that of both flat and dewetted states. This requires that

$$2\pi^2 + \frac{1}{8\pi^2}\ell^4\lambda^2 < \alpha\ell^2 + \frac{\beta}{4\pi}\ell^4\lambda^2 \tag{12}$$

and

$$2\pi^2 + \frac{1}{8\pi^2}\ell^4\lambda^2 < \alpha'\ell^2 + \frac{\beta'}{4\pi}\ell^4\lambda^2. \tag{13}$$

In other words, the membrane needs to be long enough so that capillary effects are able to overcome bending rigidity (ℓ large), but short enough so that gravity does not flatten the drop or dominate over these capillary effects (λ small).

The same graph also displays the domains of dewetting and flattening, calculated here for a typical value of the contact angle of $\theta = \pi/2$. Dewetting is the only possible state for large and rigid membranes (large ℓ and large λ) but it occurs only in a very limited range of lengths in the case of small and flexible membranes.

Experimental data on the critical size for wrapping of squares may be compared to the present two-dimensional model. Data for the minimal length for wrapping of squares are extracted from Fig. 3 of Py et al. (2007) and plotted as the open squares in Fig. 6. This figure also shows the location of the dewetting case of Section 2.2 which corresponds to that of Fig. 4, $L = 2.7$ mm, $L_{EC} = 0.8$ mm. Also shown by the thick dash is the limit between the flat and wrapped states, as derived by Py et al. (2007) using a 2-D model without gravity effects and a full numerical solution of the corresponding equilibrium equations.

3.2. Evolution to wrapping or non-wrapping

After having considered the possible final states of the drop–membrane system, we now model its evolution as the volume of liquid diminishes, as in the experiments. We assume that both the membrane and the liquid free surface have a constant uniform radius of curvature, consistent with our geometrical approximation of the final state. Let the state of the system be defined by r_1, r_2, θ_1, and θ_2, as defined in Fig. 7. The radii of curvatures of the membrane and the liquid free surface have both been scaled by the length L_{EC}, and the angles θ_1, θ_2 are half the angles of the corresponding circular arcs. Here, we assume that no dewetting occurs, so that

$$r_1 \sin\theta_1 = r_2 \sin\theta_2. \tag{14}$$

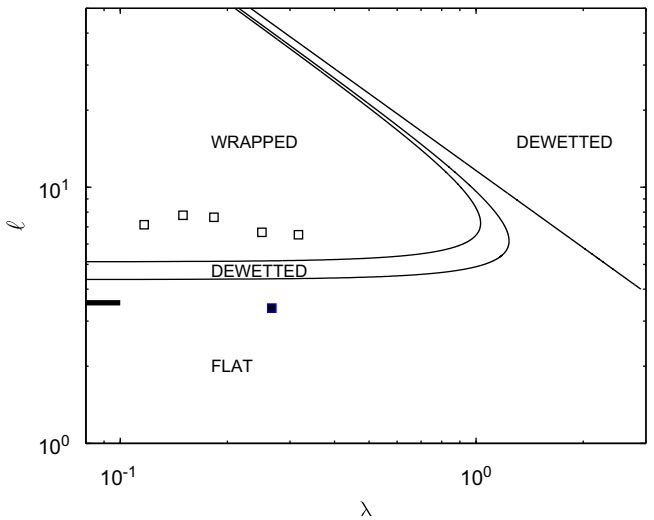

Fig. 6. Domains of wrapping, flattening and dewetting of a two-dimensional membrane in terms of dimensionless length $\ell = L/L_{EC}$ and the dimensionless elasto-capillary length $\lambda = L_{EC}/L_C$. Also shown (bold line) is the prediction of the limit between flat and wrapped states by Py et al. (2007), neglecting gravity and dewetting effects. The open squares correspond to data from Py et al. (2007). The filled square is a case of dewetting.

Please cite this article as: de Langre, E., et al., Energy criteria for elasto-capillary wrapping. Journal of Fluids and Structures (2010), doi:10.1016/j.jfluidstructs.2009.10.004

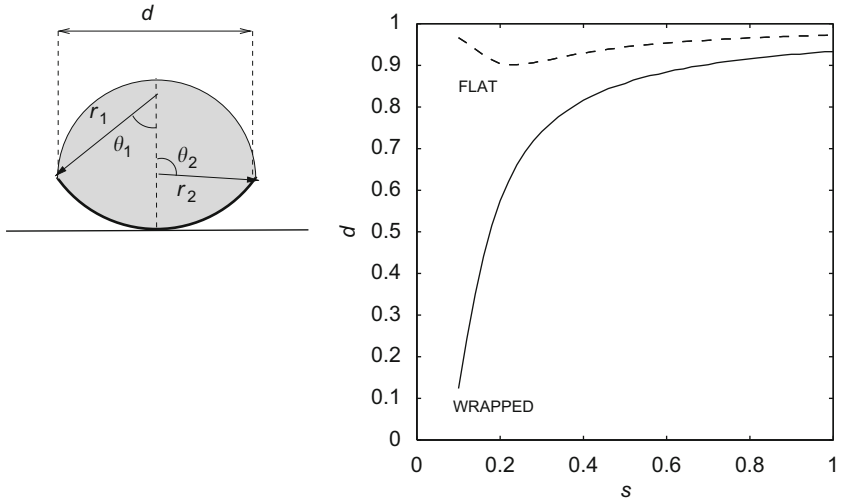

Fig. 7. Left: Geometry of the bent membrane–drop system. Right: Evolution of distance d between tips as a function of the dimensionless drop volume. Dashed line: $\ell = 3$, no wrapping. Solid line: $\ell = 5$, wrapping.

The condition that the membrane length is constant over time implies

$$2r_1\theta_1 = \ell, \tag{15}$$

and the dimensionless volume of liquid, $s = S/L_{EC}^2$ is

$$s = r_1^2(\theta_1 - \sin\theta_1\cos\theta_1) + r_2^2(\theta_2 - \sin\theta_2\cos\theta_2). \tag{16}$$

Neglecting gravity effects, for the sake of simplicity, the dimensionless total energy reads

$$\mathcal{E} = \frac{\ell^2}{2r_1^2} + 2r_2\theta_2\ell. \tag{17}$$

For a given drop volume s, the total energy of the system may be expressed as a function of only one parameter, for example θ_1. Minimizing this energy with respect to θ_1 yields the equilibrium position. This is done numerically. The distance that separates the membrane tips, $d = 2r_1\sin\theta_1$, is shown in Fig. 7 for two values of $\ell = L/L_{EC}$, first $\ell = 5$ which leads to wrapping and then $\ell = 3$ which leads to a flat state. Note the close similarity with Fig. 4 in Py et al. (2007) where the evolution is obtained from a solution of the nonlinear elastica equations. The corresponding evolutions of the geometry is shown in Fig. 8.

3.3. Mode switching during the wrapping process

As described in Section 2.1, the wrapping of a square membrane starts through a mode IV bending of the membrane and eventually switches to a mode II when the volume of liquid is further reduced (Fig. 2). We now propose a method to analyse this mode switching.

In the case of mode IV wrapping, only a part of the membrane is deformed, the central region remaining flat as sketched in Fig. 9(a). In order to keep the technical details simple, we reduce the wrapping of the triangular corners to a two-dimensional problem, modelled as the bending of a thin sheet along one direction. The simplified system conserves the amount area that is bent and the area that remains flat as sketched in Fig. 9(b) and (c). It only differs from the 2-D model of the previous section by: (a) the presence of an undeformed central region of the membrane, making up half of its width, and (b) deformed parts of width $L/\sqrt{2}$ instead of L in mode II bending.

For the sake of clarity in the comparison between the energy of the modes, we now use dimensional variables. For mode II, the dimensional energy of a square membrane as described above reads

$$\boldsymbol{E}_{\mathrm{II}} = \frac{1}{2}L^2\frac{B}{R_1^2} + LL'\gamma \tag{18}$$

Please cite this article as: de Langre, E., et al., Energy criteria for elasto-capillary wrapping. Journal of Fluids and Structures (2010), doi:10.1016/j.jfluidstructs.2009.10.004

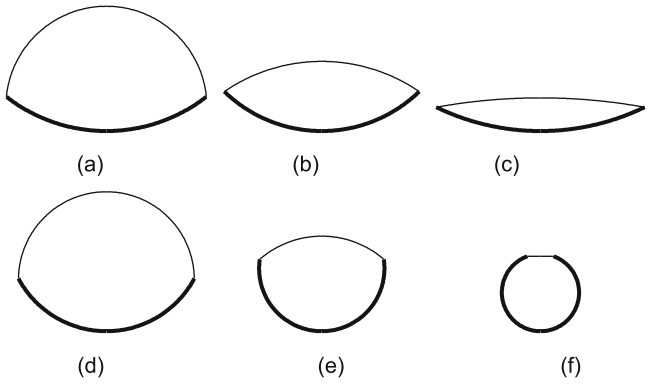

Fig. 8. Shape of the fluid surface and bent membrane derived by an energy minimization. (a–c) Evolution to a flat state, for $\ell = 3$, with $s = 0.4$, 0.2, 0.1. (d–e) Evolution to a wrapped state for $\ell = 5$, with $s = 0.4$, 0.2, 0.1.

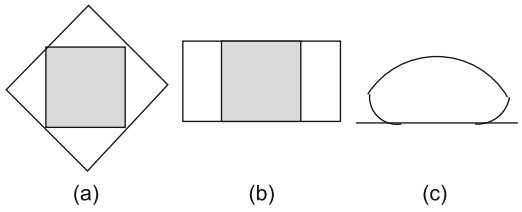

Fig. 9. (a) The three-dimensional mode IV problem of Fig. 2 is simplified into (b, c) a two-dimensional wrapping problem. The shaded area shows the undeformed part of the membrane.

with

$$L = 2R_1\theta_1, \quad L' = 2R_2\theta_2, \quad R_1\sin\theta_1 = R_2\sin\theta_2, \tag{19}$$

and these variables are related to the volume of the drop by

$$V = L[R_1^2(\theta_1 - \sin\theta_1\cos\theta_1) + R_2^2(\theta_2 - \sin\theta_2\cos\theta_2)]. \tag{20}$$

Upon eliminating R_1, R_2 and L', this reduces to

$$\frac{\boldsymbol{E}_{\mathrm{II}}}{B} = 2\theta_1^2 + \ell^2\frac{\theta_2\sin\theta_1}{\theta_1\sin\theta_2} \tag{21}$$

with

$$\frac{V}{L^3} = \frac{1}{4\theta_1^2}\left[(\theta_1 - \sin\theta_1\cos\theta_1) + \frac{\sin^2\theta_1}{\sin^2\theta_2}(\theta_2 - \sin\theta_2\cos\theta_2)\right]. \tag{22}$$

For mode IV, let us introduce the width $X = L/\sqrt{2}$ and the length $Y = L\sqrt{2}$. The dimensional energy reads now

$$\boldsymbol{E}_{\mathrm{IV}} = \frac{1}{4}XY\frac{B}{R_1^2} + XY'\gamma \tag{23}$$

with

$$Y = XR_1\theta_1, \quad Y' = 2R_2\theta_2, \quad R_1\sin\theta_1 = R_2\sin\theta_2, \tag{24}$$

and these variables are related to the volume of the drop by

$$V = X\left[R_1^2(\theta_1 - \sin\theta_1\cos\theta_1) + R_2^2(\theta_2 - \sin\theta_2\cos\theta_2) + \frac{Y}{2}R_1(1 - \cos\theta_1)\right]. \tag{25}$$

Please cite this article as: de Langre, E., et al., Energy criteria for elasto-capillary wrapping. Journal of Fluids and Structures (2010), doi:10.1016/j.jfluidstructs.2009.10.004

Upon eliminating R_1, R_2, X, Y and Y', this reduces to

$$\frac{\boldsymbol{E}_{\mathrm{IV}}}{B} = 2\theta_1^2 + \frac{\ell^2}{2}\left(\frac{\theta_2 \sin\theta_1}{\theta_1 \sin\theta_2} + \frac{\theta_2}{\sin\theta_2}\right) \tag{26}$$

with

$$\frac{V}{L^3} = \frac{(\theta_1 - \sin\theta_1\cos\theta_1)}{8\sqrt{2}\,\theta_1^2} + \frac{(\theta_2 - \sin\theta_2\cos\theta_2)}{8\sqrt{2}\sin^2\theta_2}\left(\frac{\sin\theta_1}{\theta_1} + 1\right)^2 + \frac{(1-\cos\theta_1)}{4\sqrt{2}\theta_1}. \tag{27}$$

For a given drop volume V and membrane size L the energy of each mode is obtained by minimizing $\boldsymbol{E}$ when θ_1 and θ_2 are varied under the constraint that they satisfy the equation giving the dimensionless drop volume $v = V/L^3$. The scaled energy of each mode, $\boldsymbol{E}/B$ is shown in Fig. 10 as a function of the dimensionless drop volume v. For large drop volumes, mode IV has a lower energy and can be therefore expected only to be replaced by mode II for smaller drop volumes. This switching between modes is consistent with the experimental observations of Section 2.1. It may be understood by considering that a mode IV deformation for small volumes would require the corners to bend significantly or the fluid surface to stretch, and is therefore associated with a larger energy than mode II.

3.4. A wrapping criterion

From the previous sections it appears that a two-dimensional model is relevant, at least to understand the mechanism of folding, even though the folding is a complex three-dimensional process. We now use the two-dimensional model to deduce a wrapping criterion for arbitrary shapes.

A few minor approximations are used to produce a simplified two-dimensional model that still captures the essential physics. First the length of the free liquid surface in the flat state was found to be close to L, so that one may approximate $\alpha = 1$; second, the role of gravity is small in the flat state, as can be seen by comparing β and the corresponding factor $1/2\pi$ in the energy equation. Using these approximations, the boundary between flat and wrapped states is given by

$$\ell^2 = 2\pi^2 + \frac{1}{8\pi^2}\ell^4\lambda^2. \tag{28}$$

In the limit of negligible gravity effects, $\ell = L_{EC}/L_C \ll 1$, this criterion becomes

$$\ell = \sqrt{2}\pi \simeq 4.44. \tag{29}$$

This value compares well with the value obtained by Py et al. (2007), who used nonlinear computations of a 2-D model of bending of the system in the form of an elastica and also ignored gravity, $\ell = 3.54$. This agreement can be attributed to the fact that the bending that is observed is well distributed along the elastic membrane, thus justifying the approximation of deformation with a constant radius of curvature.

Conversely, in the limit of large gravity compared to bending effects, $\ell \gg 1$, the limit is given by

$$\ell = \frac{2\sqrt{2}\pi}{\lambda}. \tag{30}$$

These two limits allow us to draw a simplified wrapping diagram, shown in Fig. 11. In dimensional terms, the criteria for wrapping become

$$\sqrt{2}\pi < \frac{L}{L_{EC}} < \frac{2\sqrt{2}\pi L_C}{L_{EC}}, \tag{31}$$

or equivalently

$$2\pi^2\frac{B}{\gamma} < L^2 < 8\pi^2\frac{\gamma}{\rho g}. \tag{32}$$

To apply these criteria to complex shapes we need to define a length scale for L. We use the folding length, $\mathcal{L}$, which we define as the maximum distance between two points of the membrane (see Fig. 12), since this length will determine

Please cite this article as: de Langre, E., et al., Energy criteria for elasto-capillary wrapping. Journal of Fluids and Structures (2010), doi:10.1016/j.jfluidstructs.2009.10.004

the easiest wrapping mode. Using this length the criteria become, in dimensional variables,

$$2\pi^2\frac{B}{\gamma} < \mathcal{L}^2 < 8\pi^2\frac{\gamma}{\rho g}. \tag{33}$$

All the cases of wrapping given in Py et al. (2007) are shown in Fig. 11, including spherical, cubic and diagonal wrapping. The corresponding elasto-capillary lengths [not given in Py et al. (2007)] are 1, 0.5 and 0.45 mm, respectively.

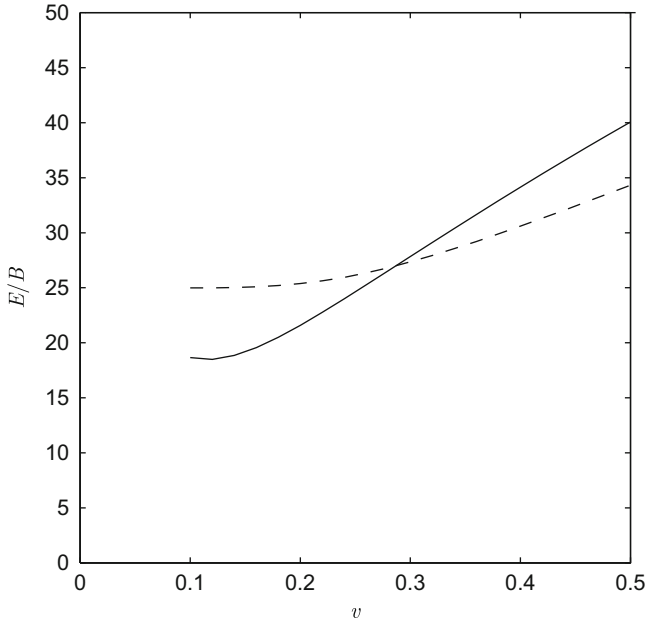

Fig. 10. Comparison of the total energies of a mode II state (—) and a mode IV state (–) for a given liquid volume v, here for $\ell = 5$. As the liquid volume is reduced, the wrapping of lowest energy switches from mode IV to II near $v = 0.3$.

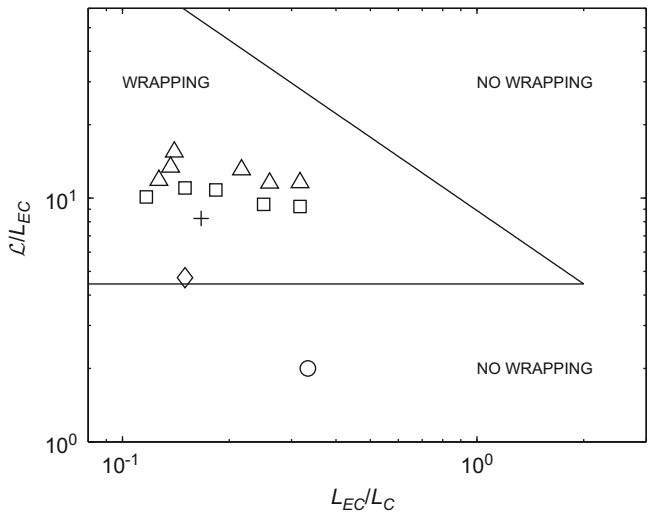

Fig. 11. A simplified criterion for wrapping as a function of the folding length $\mathcal{L}$, the capillary length $L_C = \sqrt{\gamma/\rho g}$, and the elasto-capillary length $L_{EC} = \sqrt{B/\gamma}$ (Eq. (33)). Experimental data from Py et al. (2007) showing cases of wrapping for several membrane shapes given in Fig. 12. □: squares; Δ: triangles; ○: spherical wrapping; +: cubic wrapping; and ◇: diagonal wrapping.

Please cite this article as: de Langre, E., et al., Energy criteria for elasto-capillary wrapping. Journal of Fluids and Structures (2010), doi:10.1016/j.jfluidstructs.2009.10.004

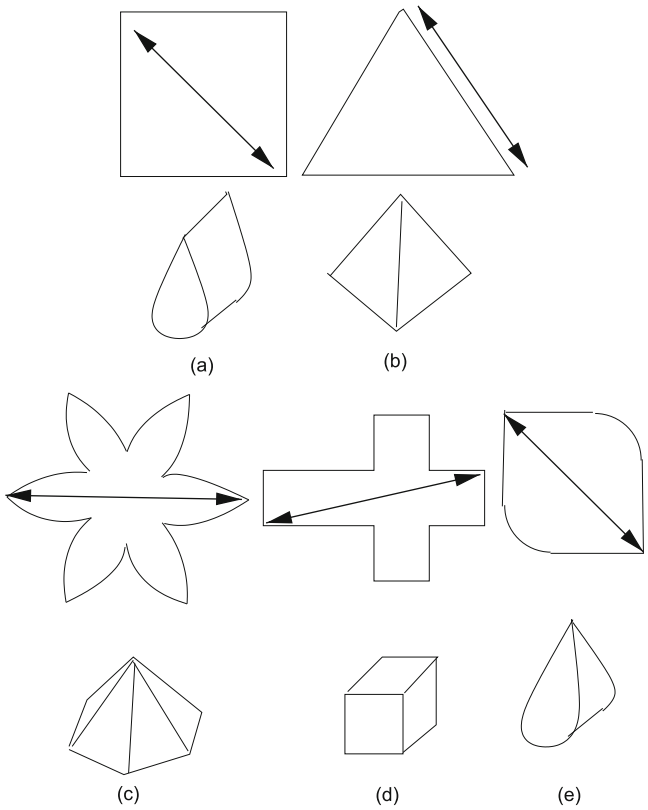

Fig. 12. Shapes of membranes and corresponding wrapped state, from Py et al. (2007). The folding length $\mathcal{L}$ is shown in each case. (a) Square, (b) triangle, (c) spherical wrapping, (d) cubic wrapping, and (e) diagonal wrapping.

All these experimental points fall in the range of possible wrapping given by Eq. (33), except the case of spherical wrapping. This may be understood by considering that the membrane "flower" shape, Fig. 12(c), is actually much more flexible than other more convex shapes.

4. Conclusions

In summary, we have shown that a model based on minimal physical ingredients can account for the experimental observations in the interactions between a liquid drop and a membrane. The model assumes a constant value for the radius of curvature of the elastic membrane and of the liquid surface, thus allowing the energy equations to be written analytically. While it is not expected that this model will capture the details of the behaviour, it allows predictions to be made based on simple calculations.

In particular, the model explains two elements in the behaviour of the "capillary origami" system which we describe in detail: Experimental observations show the possibility of dewetting of the water on the membrane for some experimental conditions. In this situation, the liquid leaves the edges of the membrane which then fails to cover the liquid–air interface. Moreover, a robust mode-switching is observed from a four-fold symmetry at early times to a two-fold symmetry at late times.

The model accounts for both of these behaviours through energy minimization arguments, at a time when a detailed modelling and simulation of these results would require major effort.

The proposed energy approach is based on the comparison between several possible configurations of the system, assuming that the observed one will be that of minimum total energy. The set of possible configurations has been here inspired by experiments. In more complex geometries, a systematic exploration of configurations that are consistent with the constraint of the system would be needed, to avoid missing important ones.

Please cite this article as: de Langre, E., et al., Energy criteria for elasto-capillary wrapping. Journal of Fluids and Structures (2010), doi:10.1016/j.jfluidstructs.2009.10.004

Further extensions can include dynamical situations in which kinetic energy plays a role, or ''Janus'' membranes which are made up of different materials. They can also account for the role of adhesion, which was neglected here. This approach can provide a useful starting point before more complex analysis is performed.

References

Halpern, D., Grotberg, J., 1992. Fluid-elastic instabilities of liquid-lined flexible tubes. Journal of Fluid Mechanics 244, 615–632.

Heil, M., 1999. Minimal liquid bridges in non-axisymmetrically buckled elastic tubes. Journal of Fluid Mechanics 380, 309–337.

Ingold, C., 1971. Fungal Spores. Their Liberation and Dispersal. Clarendon Press, Oxford.

Lau, K., Bico, J., Teo, K., Chhowalla, M., Amaratunga, G., Milne, W., McKinley, G., Gleason, K., 2003. Superhydrophobic carbon nanotube forests. Nano Letters 3 (12), 1701–1705.

Leong, T., Gu, Z., Koh, T., Gracias, D., 2006. Spatially controlled chemistry using remotely guided nanoliter scale containers. Journal of the American Chemical Society 128 (35), 11336–11337.

Madou, M., 2002. Fundamentals of Microfabrication: the Science of Miniaturization, second ed. CRC Press, Boca Raton.

Mastrangelo, C., Hsu, C., 1993. Mechanical stability and adhesion of microstructures under capillary forces. II. Experiments. Journal of Microelectromechanical Systems 2 (1), 44–55.

Ocampo, J., Vaccaro, P., Fleischmann, T., Wang, T.-S., Kubota, K., Aida, T., Ohnishi, T., Sugimura, A., Izumoto, R., Hosoda, M., Nashima, S., 2003. Optical actuation of micromirrors fabricated by the micro-origami technique. Applied Physics Letters 83 (18), 3647–3649.

Py, C., Reverdy, P., Doppler, L., Bico, J., Roman, B., Baroud, C.N., 2007. Capillary origami: spontaneous wrapping of a droplet with an elastic sheet. Physical Review Letters 98 (15), 156103.

Raccurt, O., Tardif, F. et al., 2004. Influence of liquid surface tension on stiction of SOI MEMS. Journal of Micromechanics and Microengineering 14, 1083–1090.

Smela, E., Inganas, O., Lundstrom, I., 1995. Controlled folding of micrometer-size structures. Science 268 (5218), 1735–1738.

Syms, R., Yeatmen, E., Bright, V., Whitesides, G., 2003. Surface tension-powered self-assembly of microstructures—the state-of-the-art. Journal of Microelectromechanical Systems 12, 387–417.

van Honschoten, J., Escalante, M., Tas, N., Elwenspoek, M., 2009. Formation of liquid menisci in flexible nanochannels. Journal of Colloid and Interface Science 329 (1), 133–139.

Please cite this article as: de Langre, E., et al., Energy criteria for elasto-capillary wrapping. Journal of Fluids and Structures (2010), doi:10.1016/j.jfluidstructs.2009.10.004